IMMUNOLOGY

Chimeric camel/human heavy-chain antibodies protect against MERS-CoV infection

V. Stalin Raj[1*†‡], Nisreen M. A. Okba[1*], Javier Gutierrez-Alvarez[2], Dubravka Drabek[3], Brenda van Dieren[4], W. Widagdo[1], Mart M. Lamers[1], Ivy Widjaja[4], Raul Fernandez-Delgado[2], Isabel Sola[2], Albert Bensaid[5], Marion P. Koopmans[1], Joaquim Segalés[6,7], Albert D. M. E. Osterhaus[8,9], Berend Jan Bosch[4], Luis Enjuanes[2], Bart L. Haagmans[1‡]

Middle East respiratory syndrome coronavirus (MERS-CoV) continues to cause outbreaks in humans as a result of spillover events from dromedaries. In contrast to humans, MERS-CoV–exposed dromedaries develop only very mild infections and exceptionally potent virus-neutralizing antibody responses. These strong antibody responses may be caused by affinity maturation as a result of repeated exposure to the virus or by the fact that dromedaries—apart from conventional antibodies—have relatively unique, heavy chain–only antibodies (HCAbs). These HCAbs are devoid of light chains and have long complementarity-determining regions with unique epitope binding properties, allowing them to recognize and bind with high affinity to epitopes not recognized by conventional antibodies. Through direct cloning and expression of the variable heavy chains (VHHs) of HCAbs from the bone marrow of MERS-CoV–infected dromedaries, we identified several MERS-CoV–specific VHHs or nanobodies. In vitro, these VHHs efficiently blocked virus entry at picomolar concentrations. The selected VHHs bind with exceptionally high affinity to the receptor binding domain of the viral spike protein. Furthermore, camel/human chimeric HCAbs—composed of the camel VHH linked to a human Fc domain lacking the CH1 exon—had an extended half-life in the serum and protected mice against a lethal MERS-CoV challenge. HCAbs represent a promising alternative strategy to develop novel interventions not only for MERS-CoV but also for other emerging pathogens.

INTRODUCTION

In 2012, a novel virus, termed Middle East respiratory syndrome coronavirus (MERS-CoV), was identified in humans (*1*). Six years later, more than 2000 laboratory-confirmed MERS cases, including 36% with a fatal outcome, have been reported globally. Most cases thus far originated from the Arabian Peninsula, as a result of hospital outbreaks (*2*). There is convincing evidence that dromedary camels are the primary source of MERS-CoV infection in humans. The virus isolated from camels is similar to that isolated from humans and also replicates in human cells (*3*). In addition, epidemiological and phylogenetic analyses suggest multiple introductions of MERS-CoV into the human population (*2*, *4*). This raises a great concern as MERS-CoV could continue to cause outbreaks in the near future. Effective prophylactic and therapeutic intervention strategies are therefore needed to combat this virus.

Monoclonal antibodies (mAbs) are promising candidates for the treatment and prevention of viral infections. Recently, MERS-CoV–neutralizing mAbs have been identified and characterized by several research groups, using various approaches. These antibodies have been isolated from human naïve B cells (*5*), memory B cells of MERS-CoV–infected individuals (*6*), or transgenic mice expressing human antibody variable heavy chains (VHHs) and κ light chains (*7*). All these mAbs target the receptor binding domain (RBD) of the MERS-CoV spike protein. The MERS-CoV spike protein is a structural viral component that contains the RBD, located in the S1 subunit of the protein, which binds to the MERS-CoV entry receptor dipeptidyl peptidase-4 (DPP4) (*8*). Antibodies raised against the S1 or RBD block MERS-CoV infection in vitro (*9*, *10*), and the most potent mAbs identified against MERS-CoV thus far recognize the RBD (*5*, *7*, *11*–*14*). However, production of these mAbs at a large scale is costly and requires a long developmental process, and relative large quantities might be needed to protect humans against a viral infection (*15*). Alternatively, antibody engineering technologies allow the cloning of variable regions of mAbs for expression in *Escherichia coli* or yeast to produce large amounts of recombinant antibody fragments (*16*). To date, 68 therapeutic mAbs have been licensed, of which 7 are chimeric antibodies (*17*).

Heavy chain–only antibodies (HCAbs) are naturally produced in camelid species (*18*). These antibodies are dimeric and do not contain a light chain, and their antigen recognition region is solely formed by the VHH region termed single-domain antibody fragment. This fragment is about 14 kDa in size, is relatively stable, and can be produced with high yields in prokaryotic systems (*18*, *19*). Camelid VHHs have long complementarity-determining region 3 (CDR3) loops, capable of binding to unique epitopes not accessible to conventional antibodies (*20*). Because of these beneficial properties, VHHs have been exploited for a range of biotechnological applications, including diagnostics, therapeutics, and fundamental research (*21*, *22*). The recent preclinical success of a VHH that blocks von Willebrand factor–mediated platelet aggregation (*23*) shows their

[1]Department of Viroscience, Erasmus Medical Center, Rotterdam, Netherlands. [2]Department of Molecular and Cell Biology, National Center for Biotechnology–Spanish National Research Council (CNB-CSIC), Madrid, Spain. [3]Department of Cell Biology, Erasmus Medical Center, Rotterdam, Netherlands. [4]Virology Division, Department of Infectious Diseases and Immunology, Faculty of Veterinary Medicine, Utrecht University, Utrecht, Netherlands. [5]Institut de Recerca i Tecnologia Agroalimentàries (IRTA), Centre de Recerca en Sanitat Animal [CReSA, IRTA–Universitat Autònoma de Barcelona (UAB)], Campus de la UAB, 08193 Bellaterra, Spain. [6]UAB, CReSA (IRTA-UAB), Campus de la UAB, 08193 Bellaterra, Spain. [7]Departament de Sanitat i Anatomia Animals, Facultat de Veterinària, UAB, 08193 Bellaterra, Spain. [8]Artemis One Health, Utrecht, Netherlands. [9]Center for Infection Medicine and Zoonoses Research, University of Veterinary Medicine, Hannover, Germany.
*These authors contributed equally to this work.
†Present address: School of Biology, Indian Institute of Science Education and Research Thiruvananthapuram (IISER-TVM), Kerala, India.
‡Corresponding author. Email: stalin@iisertvm.ac.in (V.S.R.); b.haagmans@erasmusmc.nl (B.L.H.)

therapeutic potential. VHHs may also efficiently prevent entry of viruses into host cells (*24*). Chimeric HCAbs, which have the camel VHH and the human Fc portion (lacking the CH1 exon as in camel HCAbs), allow them to interact with human effector cells and complement cascade factors (*15*).

Several studies have demonstrated the presence of high levels of MERS-CoV–specific neutralizing antibodies (mean virus neutralization titer ≈ 1000) in dromedary camels in the Middle East and Africa (*25–27*). Therefore, next to human mAbs, characterization of MERS-CoV–neutralizing VHHs from dromedary camels could serve as an alternative strategy to develop neutralizing antibodies. Here, we report the identification and characterization of neutralizing VHHs against MERS-CoV from immunized dromedary camels and demonstrate the prophylactic activity of camel/human chimeric HCAbs in a MERS-CoV transgenic mouse model.

RESULTS

Identification of MERS-CoV–specific VHHs from a dromedary camel bone marrow complementary DNA library

First, we identified MERS-CoV–neutralizing VHHs by direct cloning and screening of VHH complementary DNA (cDNA) libraries derived from bone marrow cells (given the high frequency of specific plasma cells) rather than using B cells from peripheral blood of immunized animals (Fig. 1). Bone marrow was obtained from two dromedary camels immunized with modified vaccinia virus encoding the MERS-CoV spike protein and subsequently challenged with live MERS-CoV (*28*). At the time of sampling, MERS-CoV–neutralizing antibodies were detected at very high levels (titer > 10,000) in the sera of these dromedaries (Fig. 2A). Subsequently, VHH-specific primers (*29*) were used to amplify a VHH library from the bone marrow cDNA by nested polymerase chain reaction (PCR) (fig. S1, A to C).

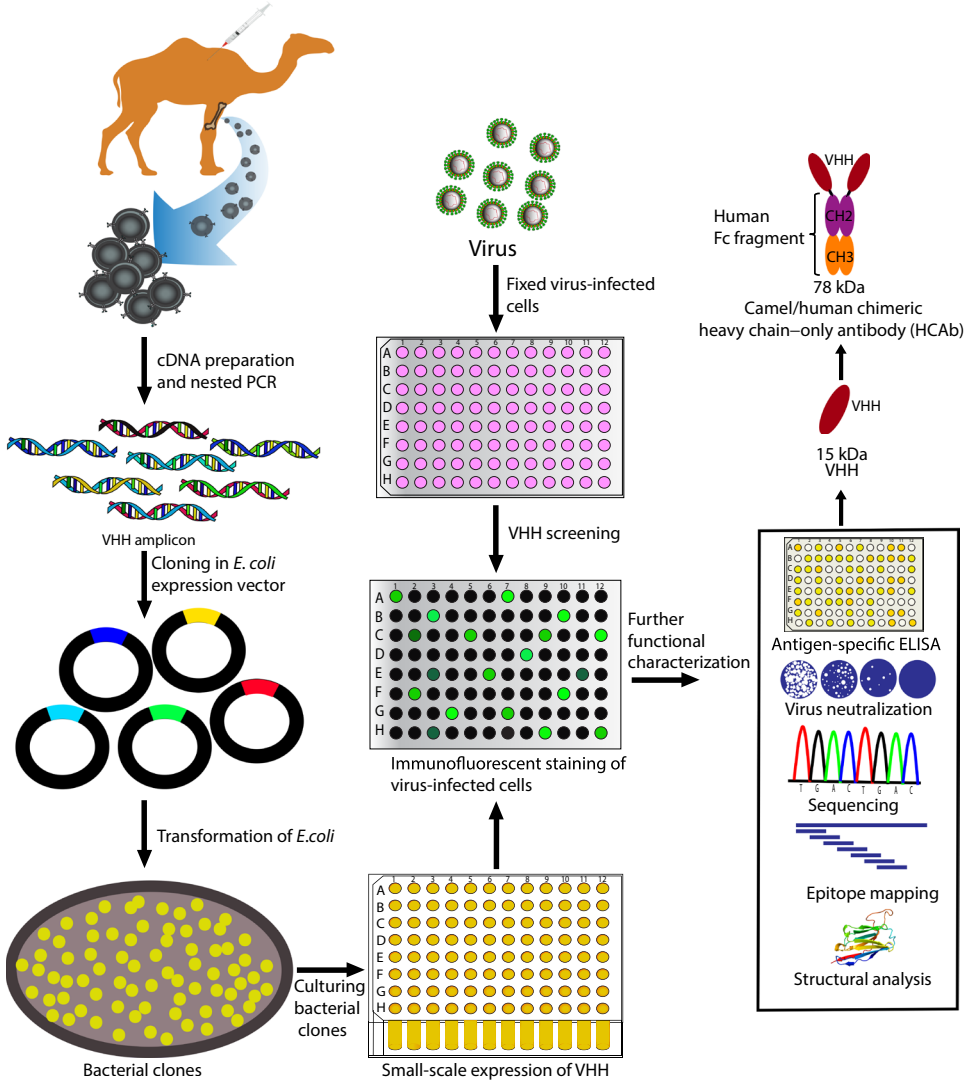

Fig. 1. Schematic overview of VHH identification by direct cloning using bone marrow from immunized dromedary camels. Immunized dromedary camels were anesthetized, and bone marrow aspirations were performed. After total RNA isolation and first-strand cDNA synthesis, VHH genes were amplified and cloned into a prokaryotic expression vector (pMES4) and transformed into *E. coli* WK6. Individual clones were grown overnight in 96-deep-well plates, during which they expressed the VHHs in the periplasm. Next, crude VHHs were released from the periplasm by freeze-thawing the bacterial pellet. Crude VHHs were used for immunofluorescent staining on virus-infected cells. Immunofluorescent positive clones were further characterized for their genetic makeup, specificity, and potency by sequencing, antigen-specific enzyme-linked immunosorbent assay (ELISA), virus neutralization assay, epitope mapping, and structural analysis. Finally, potent VHHs were produced as camel/human chimeric single chain–only antibodies.

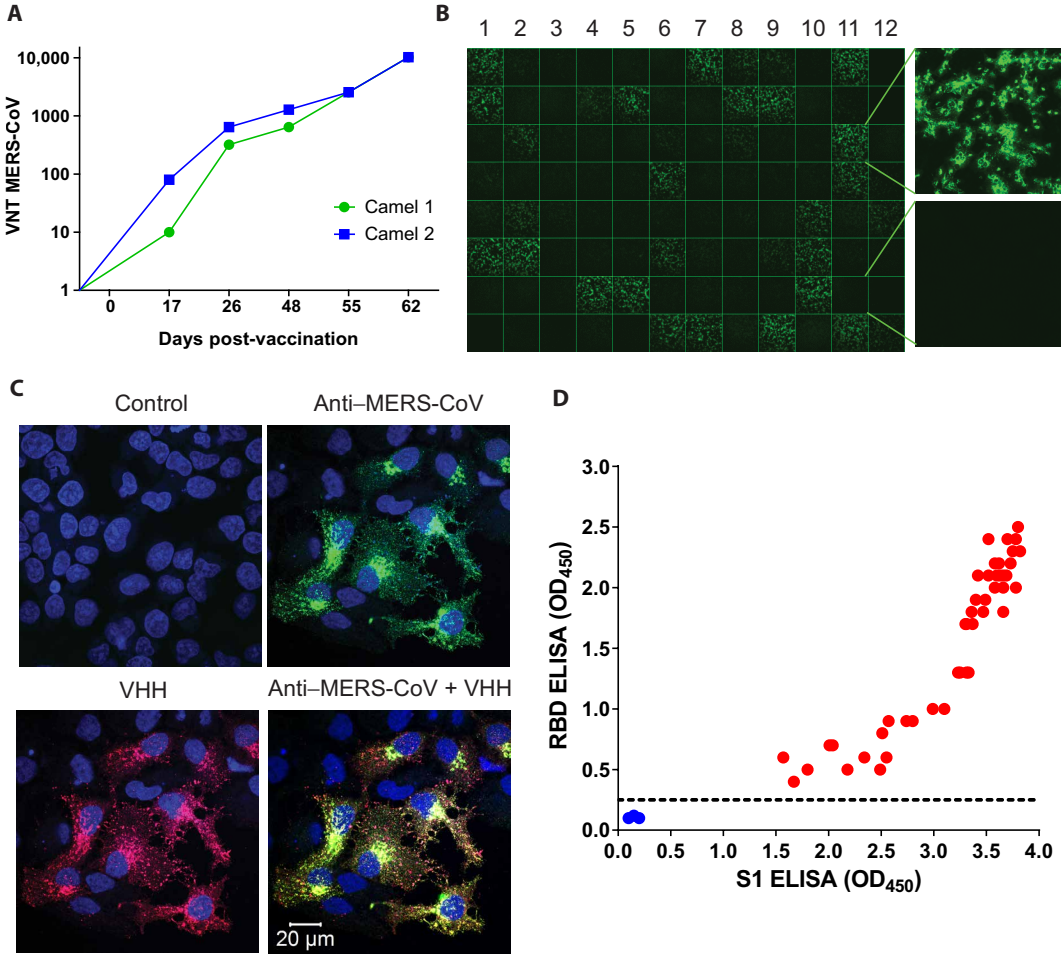

Fig. 2. Identification of VHHs directed against the spike (S) protein of MERS-CoV. (**A**) Virus-neutralizing antibody titers (VNT) of sera from two dromedary camels immunized with MVA expressing the MERS-CoV-S (MVA-S) and challenged with MERS-CoV. (**B**) Immunofluorescent staining of MERS-CoV–infected Huh-7 cells with crude VHHs. Each square represents staining of an individual VHH. (**C**) Immunofluorescent staining of MERS-CoV–infected Huh-7 cells with rabbit serum (anti–MERS-CoV) or crude VHHs and overlay. (**D**) Correlation of the S1-specific ELISA and the RBD-specific ELISA for the 46 MERS-CoV–neutralizing VHHs (red dots) and control VHHs indicated as blue dots (Spearman correlation $r = 0.9258$; $P < 0.0001$; 95% confidence interval, 0.8677 to 0.9589). OD, optical density.

After gel purification, PCR products were directly cloned into the dephosphorylated prokaryotic expression vector pMES4, tagging the VHHs with six histidine amino acids at the C terminus (*29*). To obtain a high-diversity repertoire of VHHs, we reduced the number of amplification cycles. The ligated VHH plasmid library was transformed into *E. coli* strain WK6 and plated on ampicillin nutrient agar plates without preculturing the bacteria in nutrient medium. A total of 560 VHH clones (225 from camel 1 and 335 from camel 2) were obtained in a single transformation event, and grown individually in 96-deep-well plates. Periplasmic expression of recombinant VHHs was induced by isopropyl-β-D-thiogalactopyranoside (Fig. 1). VHHs were purified from the periplasm as a crude extract (*30*), and expression was verified using SDS–polyacrylamide gel electrophoresis (PAGE) analysis (fig. S1D).

Next, we used formalin-fixed and permeabilized virus-infected cells [either MERS-CoV–infected or severe acute respiratory syndrome coronavirus (SARS-CoV)–infected] to select for MERS-CoV–specific VHHs using immunofluorescent staining. Crude periplasmic VHH extracts were incubated on the infected cells, and VHH cell binding was visualized with a fluorescently labeled anti-histidine antibody as a secondary antibody. All 560 VHH clones were screened by confocal microscopy (Fig. 2B). We obtained 204 MERS-CoV–reactive VHHs (41.7% from camel 1 and 58.3% from camel 2), of which none reacted to SARS-CoV–infected cells. To confirm the specificity of the VHHs for MERS-CoV, we randomly selected several clones for double staining of MERS-CoV–infected cells using a rabbit anti–MERS-CoV serum, revealing that these VHHs exclusively targeted MERS-CoV–infected cells (Fig. 2C).

Blocking of RBD binding to receptor DPP4 by MERS-CoV spike-specific VHHs in vitro

To test whether the VHHs identified in our study recognized the RBD or other parts of the S1, we performed MERS-CoV S1– and MERS-CoV RBD–specific ELISAs. Out of 204 MERS-CoV–reactive VHHs, 188 (92.15%) were directed against the MERS-CoV S1 subunit, of which 46 VHHs (22.5%) blocked the binding of recombinant S1 to the MERS-CoV receptor present on Huh-7 cells (fig. S2). All these in vitro blocking VHHs were directed against the RBD (Fig. 2D).

Next, we selected all blocking VHHs for further characterization. The VHH clone p2E6 (negative for immunofluorescent staining and S1 ELISA) was used as the negative control. Using a MERS-CoV plaque reduction neutralization test (PRNT), we estimated the virus neutralization capacity for each VHH. Except for the control VHH-p2E6, all tested VHHs inhibited MERS-CoV entry at varying concentrations ranging from 100 to 900 pM ($PRNT_{90}$; table S1). VHHs with high neutralizing capacity (VHH-1, VHH-4, VHH-83, and VHH-101) were selected for further characterization.

We obtained sequences from all 46 blocking VHHs. Because CDR3 is known to be of most importance for the interaction with the antigen, the assumption was made that VHHs with the identical CDR3 would recognize the same epitope. Overall, 33 VHHs had different CDR3 sequences ranging in length from 16 to 20 amino acids (fig. S3). Phylogenetic analysis of these sequences revealed considerable diversity among the different VHH clones and showed that the selected VHHs formed 14 different clusters with different CDR3 sequences (fig. S4). All sequences contained the characteristic VHH tetrad, except clone 10 that, at amino acid positions 37, 45, and 47, shows VH characteristics (valine, leucine, and tryptophan). The best MERS-CoV–neutralizing VHHs (VHH-1, VHH-4, VHH-83, and VHH-101) had different CDR3 sequences (fig. S4).

VHHs bind to MERS-CoV spike protein with high affinity

Subsequently, the best four neutralizing VHHs and the control VHH-p2E6 were selected for large-scale production and purification. We obtained high quantities (5 to 30 mg) of pure (>95%) His-tag affinity-purified VHHs from 1 liter of bacterial culture (fig. S5A). Mixing these VHHs with recombinant MERS-CoV spike S1 protein generated VHH-spike complexes, as observed by nonreducing PAGE analysis (fig. S5B). In addition, the equilibrium dissociation constant (K_d) between the VHH and spike protein of these four VHHs was relatively low, with K_d values ranging from 1 to 0.1 nM, indicating high-affinity binding (fig. S6, A and B).

Neutralization of MERS-CoV by VHHs and camel/human chimeric HCAbs

Next, we tested the neutralizing activities of these VHHs in vitro by PRNT. All four VHHs were confirmed to neutralize MERS-CoV with high efficiency, with $PRNT_{50}$ values ranging from 0.0014 to 0.012 μg/ml (93 to 800 pM), while no inhibition was observed using the control VHH-p2E6 at high concentration (>1.0 μg/ml; 67 μM; Fig. 3A). Because of their small size, VHHs are rapidly cleared from the circulation (*30*, *31*). Therefore, we additionally produced the four VHHs as camel/human chimeric HCAbs by C-terminal tagging the VHHs with the Fc part of human immunoglobulin G2 (IgG2) (containing the hinge and CH2 and CH3 exons) (Fig. 1, right). These HCAbs (HCAb-1, HCAb-4, HCAb-83, and HCAb-101) form homodimers of about 78 kDa in size and exhibit approximately the same neutralizing capacity as the monomeric VHHs in vitro (Fig. 3B). Moreover, using an S1-specific ELISA, we could detect HCAb binding at even lower concentrations, down to 0.00019 μg/ml (2.5 pM; Fig. 3C).

Epitope mapping of four potent MERS-CoV–neutralizing VHHs

To map the VHH binding epitopes, we first tested the binding of the four different VHHs to recombinant S1 protein using ForteBio's Octet system. As shown in fig. S7, all four VHHs competed for a single epitope. Subsequently, we used a set of recombinant S1 proteins that contain single amino acid mutations present in spike proteins of MERS-CoV field isolates, located within the receptor binding subdomain (residues 483 to 566) of the RBD that engages DPP4. MERS-CoV polyclonal antibodies, an irrelevant VHH, and four VHHs were then tested for their ability to bind to these S1 variants. MERS-CoV polyclonal antibodies, but not the control VHH-p2E6, bound to all variants (Fig. 4, A and B), whereas the four MERS-CoV–specific VHHs did not bind to the D539N variant and differed in their binding to the other variants. VHH-1 also did not bind to variant E536K, whereas VHH-4 and VHH-101 showed partial binding to three additional variants (I529T, V534A, and E536K) (Fig. 4, C to F). These data show that all four VHHs bind an epitope in the receptor binding subdomain

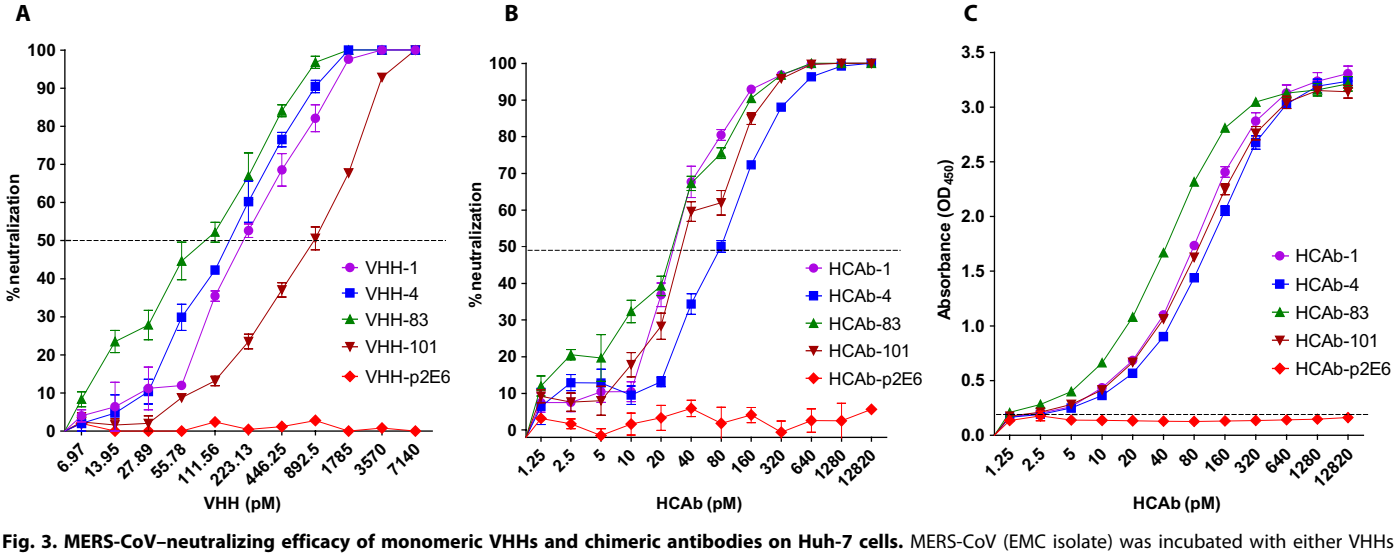

Fig. 3. MERS-CoV–neutralizing efficacy of monomeric VHHs and chimeric antibodies on Huh-7 cells. MERS-CoV (EMC isolate) was incubated with either VHHs (monomer), chimeric antibodies, or controls at various concentrations for 1 hour and then the mix was transferred on Huh-7 cells. Cells were fixed 8 hours after infection and stained using rabbit polyclonal antibodies. The PRNT titer was calculated on the basis of a 50% or greater reduction of infected cells ($PRNT_{50}$). (**A**) PRNT assay for VHH monomer. (**B**) PRNT for camel/human chimeric heavy-chain antibodies. Experiments were performed at least two times in triplicate, data from an experiment were presented, and error bars show SEM. (**C**) MERS-CoV S1 ELISA using different HCAbs. The optical density at 450 nm was presented in triplicate, with error bars showing SEM.

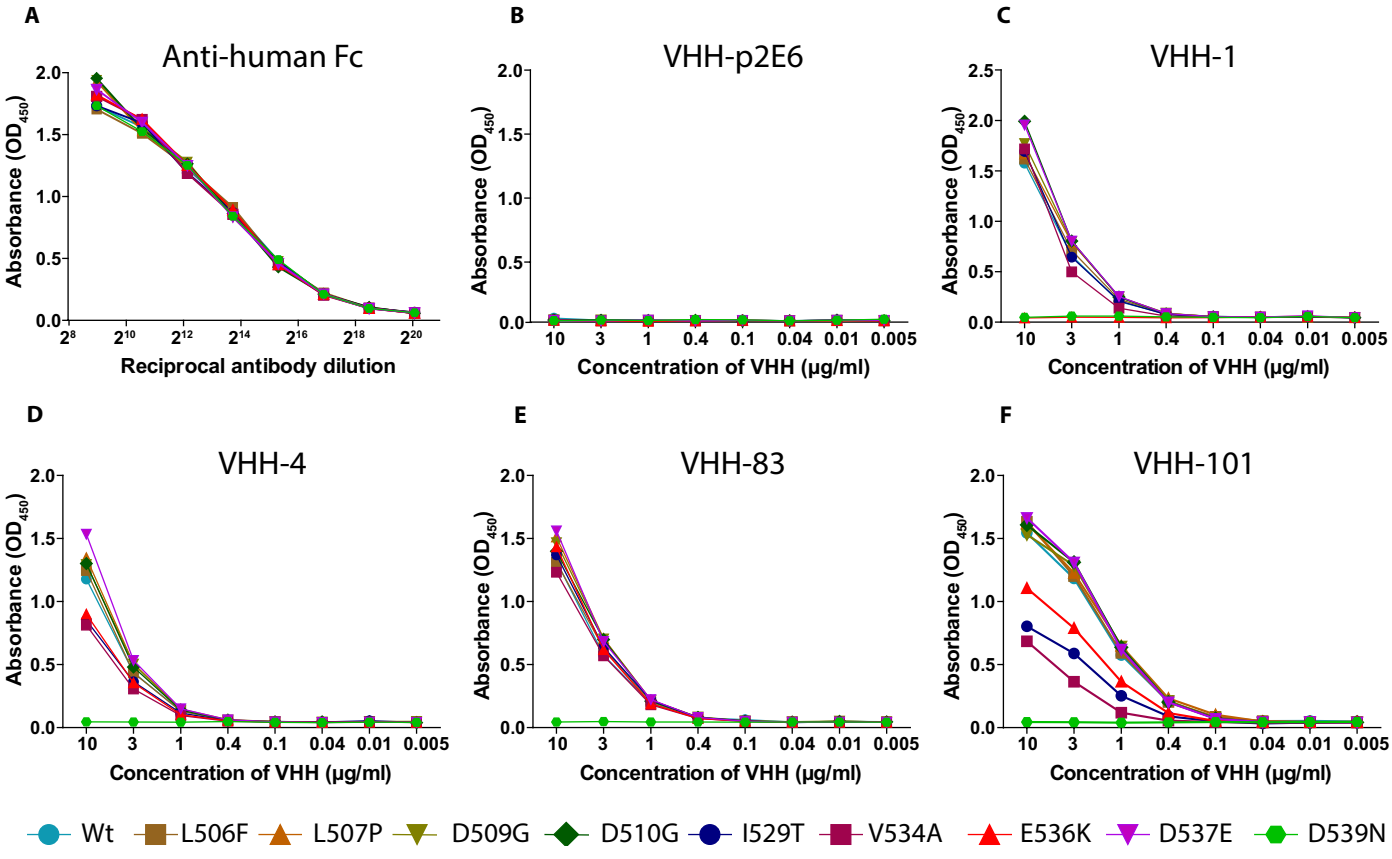

Fig. 4. Effect of MERS-CoV RBD residue substitution on VHH binding. Binding efficiency of VHHs to the wild-type and mutant forms of viral spike glycoprotein was analyzed by ELISA. The binding efficiency was calculated on the basis of optical density (OD_{450}) of mutant protein versus that of the wild-type spike. (**A**) Anti-human IgG polyclonal antibodies were used to corroborate equivalent coating of the S1-hFc variants. (**B**) One irrelevant VHH (VHH-p2E6) lacked binding to wild-type and mutant proteins. (**C**) VHH-1. (**D**) VHH-4. (**E**) VHH-83. (**F**) VHH-101.

that is partially overlapping, consistent with the binding competition analysis (fig. S7). The RBD residues D537, D539, Y540, and R542 are important for the virus to bind to its cellular receptor DPP4 (*32*, *33*). Because all four VHHs did not bind to the D539N variant, this suggests that these VHHs neutralize MERS-CoV most likely by blocking its binding to its cellular receptor. Despite several attempts, we were not able to identify MERS-CoV escape variants in vitro. Because of the best neutralizing capacity and epitope recognition, we selected VHH-83 and HCAb-83 for further in vivo testing.

In vivo efficacy of VHH-83 and HCAb-83

To test the prophylactic efficacy of VHH-83 or HCAb-83 in vivo, we used the K18 transgenic mouse model (*34*). In our first experiment, mice were given VHH-83 or an irrelevant VHH control (p2E6) at 20 or 200 μg per mouse (nine mice per group) by intraperitoneal injection 6 hours before intranasal infection with a lethal dose of MERS-CoV (EMC isolate). Mice that received VHH-83 lost weight and died within 7 days post-inoculation (dpi), as well as those injected with the control VHH (fig. S8).

Next, we tested HCAb-83 or the control HCAb-p2E6 using a similar experimental setup. Mice treated with 200 μg of HCAb-83 gained weight (Fig. 5A), and all mice survived (Fig. 5B). In contrast, control HCAb-p2E6–treated groups lost weight and died within 7 dpi (Fig. 5, A and B). Gross pathological changes (Fig. 5C), mononuclear cell infiltration, and alveolar edema (Fig. 5E) were observed in the lungs of control HCAb-p2E6–treated mice on day 4 after inoculation. Whereas low doses (20 μg) of HCAb-83–treated mice were only partially protected on the basis of the observed reduction of pathological abnormalities on 4 dpi (Fig. 5F), the lungs of high-dose HCAb-83–treated mice showed no pathological changes at any time point tested (Fig. 5G). In addition, no infectious virus could be isolated from the lungs of these mice, while high viral titers were observed in the low dose– and control HCAb–treated mice (Fig. 5H).

Pharmacokinetics of HCAb-83

We also evaluated the pharmacokinetics of VHH and HCAb in the sera of mice treated with either VHH-83 or HCAb-83. First, we estimated the presence of MERS-CoV–neutralizing activity in sera obtained 2 days after treatment. No neutralization of the virus was observed in the sera of VHH-83– or control VHH-p2E6–treated mice (Fig. 6A), consistent with the reported rapid clearance of small VHH domains from the circulation (*31*). Significant levels of neutralizing antibodies (mean titer, 1024) were observed in the sera of mice treated with 200 μg of HCAb-83 and, to a limited extent, in low dose–treated mice (mean titer, 64; Fig. 6A). Second, we tested the presence of circulating HCAb-83 in the sera obtained at various time points after injection (0, 2, 4, and 8 days after treatment) by ELISA. As shown in Fig. 6B, 200 μg of HCAb-83–treated mice still had high levels of HCAb-83 8 days after treatment, with an apparent serum half-life of approximately 4.5 days.

DISCUSSION

VHHs are small in size; have high stability, solubility, and affinity; and efficiently recognize antigens. They have many potential biomedical applications including the treatment of cancer, autoimmune diseases, and virus infections (*18*, *19*, *22*, *24*, *31*). Moreover, VHHs are gaining much attention in the field of diagnostics and therapeutics for viral diseases. They have been used for the detection of viruses, such as Marburg virus, human immunodeficiency virus (HIV), influenza virus, dengue virus, and norovirus (*22*, *24*). VHHs also block virus attachment to the host cells in respiratory syncytial virus, influenza virus, hepatitis B virus, rotavirus, and HIV infections (*22*, *24*). Some VHHs inhibit viral RNA transcription or nuclear import of viral ribonucleoproteins (*35*). Here, we have shown that MERS-CoV–neutralizing VHHs can be obtained from immunized dromedary camels that were

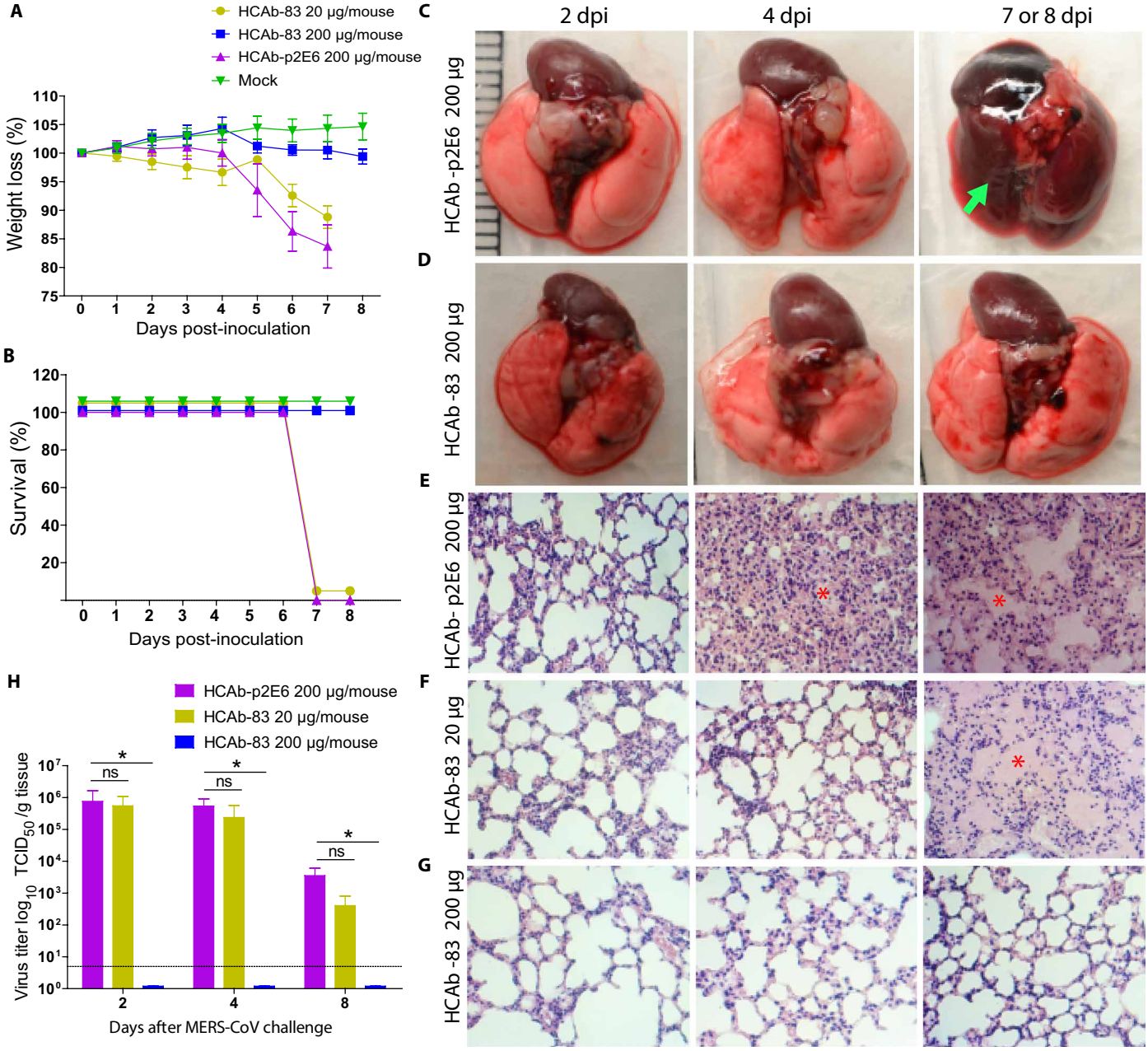

Fig. 5. Prophylactic efficacy of HCAb-83 in K18 mice challenged with a lethal dose of MERS-CoV. K18 mice (n = 9 per group) were injected intraperitoneally with HCAb-83 (20 or 200 μg per mouse) 6 hours before challenge with 10^5 $TCID_{50}$ (median tissue culture infectious dose) of MERS-CoV (EMC isolate). HCAb-p2E6 was injected as a negative control (n = 9). Mice were monitored daily for (**A**) weight loss and (**B**) mortality. Weight loss is expressed as a percentage of the initial weight. Lungs were collected at days 2, 4, and 8 (n = 3 per time point) or from mice that died in between and were processed to asses gross pathology (**C** and **D**) and histopathological changes (**E** to **G**). Gross pathology of one representative animal that died at day 7 when treated with HCAb-p2E6 is indicated by a green arrow (C, right). Lung sections were stained with hematoxylin and eosin. Asterisk indicates alveolar edema. (**H**) MERS-CoV viral titer quantitation of infected lungs at days 2, 4, and 8 (n = 3 per time point) after infection (n = 3 mice per time point); one-way ANOVA. *P < 0.05. ns, not significant.

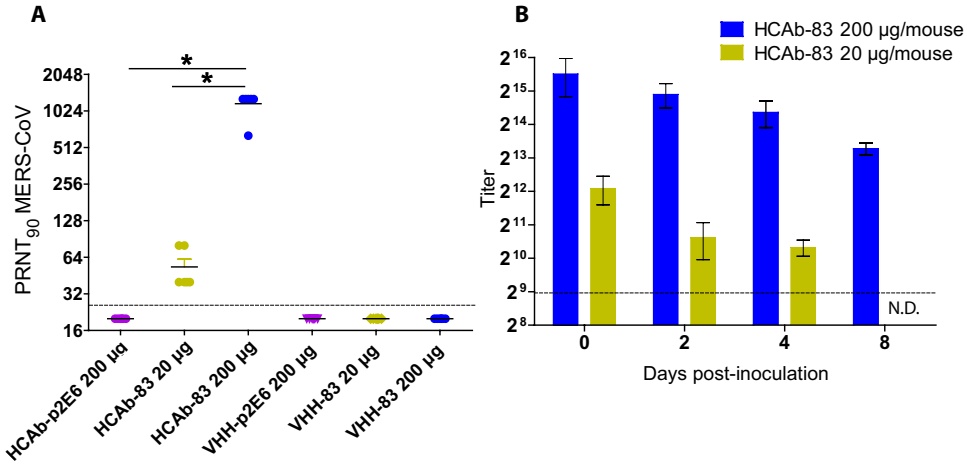

Fig. 6. Pharmacokinetics of HCAb-83 in K18 transgenic mice. (**A**) MERS-CoV PRNT performed on sera of mice collected 2 days after treatment with VHH-83, HCAb-83, or controls. The PRNT titer was calculated on the basis of a 90% reduction in the infected cell counts. Statistically significant differences were observed between groups HCAb-p2E6 200 µg, HCAb-83 200 µg, and HCAb-83 20 µg (one-way ANOVA test, *$P < 0.05$). (**B**) Detection of HCAbs in the sera of HCAb-83–treated mice at various time points using ELISA. N.D., not determined.

challenged with MERS-CoV. The engineered camel/human chimeric HCAbs were highly stable in mice, and prophylactically treated mice were fully protected from MERS-CoV infection upon challenge with live virus.

Naturally infected dromedary camels have remarkably high levels of neutralizing antibodies against MERS-CoV (*25*, *36*). We used dromedaries that showed high levels of neutralizing antibodies in their sera and identified MERS-CoV–neutralizing VHHs by direct cloning from a VHH cDNA library using bone marrow, a major source of highly enriched long-lived antibody-producing plasma cells. After immunization, antigen-stimulated B cells undergo affinity maturation in germinal centers of secondary lymphoid organs, where they differentiate into plasma cells that secrete antibodies. Significant portion of long-lived plasma cells migrate to the bone marrow. A small portion of plasma cells reside in the lymphoid organs, but these are often short-lived (*37*, *38*). In mice, 8 days after boost immunization with ovalbumin, about 10 to 20% of the antigen-specific plasma cells migrate from secondary lymphoid organs to the bone marrow (*39*). In particular, bone marrow plasma cells are long-lived and are thus suitable for maintaining antibody levels in the serum for an extended period, which plays a significant role in pathogen neutralization and humoral immune responses (*40*). The number of S1-specific clones found in the VHH library generated from vaccinated and infected camels (188 of 560 clones; 33.5%) was much higher compared to nonvaccinated infected camels (12 of 496 clones; 2.4%), suggesting that the vaccination and challenge protocol used in this study had a major impact on the frequency of S1-specific B cells detected in the bone marrow.

Camelid species have naturally occurring HCAbs. These antibodies contain long CDR3 sequences (*20*), which allow them to interact with unique and even recessed epitopes that may not be recognized by conventional antibodies (*20*, *41*). We identified 46 MERS-CoV–neutralizing VHHs, of which 4 bound to the RBD of the spike protein with high affinity and neutralized MERS-CoV infection at picomolar concentrations. VHH-83 showed a neutralizing capacity down to a concentration of 30 pM ($PRNT_{50}$), making it more potent than the most potent mAbs described thus far (*7*, *42*). However, direct comparisons between different antibodies would require determining the exact differences in vitro. Competition and spike protein binding assays showed that the four VHHs competed for binding to an overlapping epitope on the RBD, which partially overlaps with the RBD-DPP4 interface. Binding assays using variant recombinant spike proteins revealed that all four VHHs bound to wild-type spike protein but not to a D539N-mutant protein. Amino acids E536, D537, and D539 are negatively charged residues on the surface of the RBD, which interact with three positively charged residues on the outer surface of the DPP4 (*32*, *33*). This indicates that the four VHHs can prevent virus attachment and entry. Given the critical role of these amino acids in the DPP4-virus interaction, viral escape mutants without loss of fitness are less likely to develop (*32*, *33*). This could be the reason why we did not identify HCAb-83 escape variants in vitro. However, further (structural) studies are needed to pinpoint all RBD-VHH contact residues involved.

Next, we produced the four VHHs as HCAbs, which showed threefold enhanced MERS-CoV–neutralizing capacity in comparison to the monomeric VHHs in vitro ($PRNT_{50}$, 30 pM). In contrast to VHH-83, mice prophylactically treated with 200 µg of HCAb-83 were fully protected from weight loss and death upon challenge with live virus. No infectious virus was detected in the lungs of these mice, and protection correlated with the presence of sustained high levels of HCAbs-83 in the sera of mice. In addition, most in vivo studies testing mAbs to MERS-CoV showed only reduced MERS-CoV replication (two to four log reductions in lung virus titer) or complete protection only at higher doses used (1000 µg per mouse) (*6*, *7*, *13*). The high level of neutralizing activity of HCAb-83 ($PRNT_{50}$, 30 pM) could be due to the different antigen recognition pattern of camelid HCAbs. Recent studies also revealed the importance of long CDR3 sequences from bovine antibodies raised against HIV in cross-neutralization against different viral serotypes (*43*). The therapeutic efficacy of HCAb-83 still needs further evaluation, but given the limited therapeutic efficacy of other mAbs against acute respiratory infections such as respiratory syncytial virus in humans (*44*), prophylactic administration of antibodies may also be preferred to contain outbreaks of MERS-CoV.

Apart from direct neutralization, antibodies may also play a role in mediating effector functions such as complement-dependent cytotoxicity and antibody-dependent cell-mediated cytotoxicity (*16*). HCAb-83 has an Fc domain of human IgG2, which has limited effector function in vivo (*17*), suggesting that the observed protection in mice could be mainly due to the neutralizing activity. Therefore, additional

studies need to evaluate whether the potency of HCAb-83 may be increased further by replacing the IgG2 Fc with the IgG1 Fc or by combination with other antibodies targeting different epitopes.

In summary, we identified and characterized potent HCAbs that neutralized MERS-CoV in vitro and in vivo. Because of their high affinity, in vivo stability, and efficacy, these HCAbs may be used as a prophylaxis for MERS-CoV.

MATERIALS AND METHODS

Immunization

One female (6-month-old) and one male (8-month-old) healthy dromedary camels (*Camelus dromedarius*), negative for antibodies against MERS-CoV and modified vaccinia virus Ankara (MVA), were obtained from the Canary Islands and housed in biosecurity level 3 (BSL-3) facilities [Centre de Recerca en Sanitat Animal (CReSA)], as described previously (*28*). Experimental procedures were approved by the local Ethics Committee of the Autonomous University of Barcelona (number 8003). Both animals were immunized twice with a 4-week interval with 10^8 plaque-forming units of MVA-S via both nostrils and intramuscularly in the neck of the animals. After the second immunization, both animals were anesthetized with midazolam (5 mg/ml) and inoculated with 10^7 $TCID_{50}$ MERS-CoV in 3 ml of phosphate-buffered saline (PBS) intranasally in both nostrils using a laryngo-tracheal mucosal atomization device (*45*). Blood samples were taken at different dpi. On day 14 after inoculation, both animals were anesthetized and femoral bone marrow samples (about 1 cm^3) were collected next to the epiphysis and placed, each, in tubes containing 3.6 ml of ice-cold fetal calf serum. Specimens were gently crushed with a 1-ml tip and homogenized by slow up and down pipetting. After 10-min incubation on ice, 400 µl of dimethyl sulfoxide was mixed into each tube, and the preparation was dispensed into 2-ml cryovials discarding debris and slurs and stored at −135°C.

Protein expression

The recombinant S1-Fc fusion proteins were produced as described previously (*46*). Briefly, plasmids encoding MERS-CoV S1-Fc or MERS-CoV RBD-Fc were generated by ligating a fragment encoding the S1 subunit (GenBank accession number AFS88936; residues 1 to 747) or RBD (residues 358 to 588) 3′ terminally to a fragment encoding the Fc domain of human IgG1 into the pCAGGS expression vector. Plasmids encoding S1-Fc variants with single amino acid substitutions were generated by site-directed mutagenesis. S1-Fc fusion proteins were expressed by transfection of the expression plasmids into human embryonic kidney (HEK)–293T (CRL-11268, American Type Culture Collection) cells and affinity-purified from the culture supernatant using Protein A-Sepharose beads (GE Healthcare).

Estimation of antibody/VHH titers

MERS-CoV–specific antibody titers were measured by ELISA. First, 96-well plates were coated with MERS-CoV S1 or MERS-CoV RBD proteins at 1 µg/ml in PBS (pH 7.4) and incubated overnight at 4°C. Wells were then washed three times with PBS, blocked with 10% normal goat serum in PBS, and incubated at 37°C for 30 min. Dromedary camel sera or VHHs were serially diluted in PBS, 100 µl was added per well, and plates were incubated at 37°C for 1 hour. Next, plates were washed three times in PBS containing 0.05% Tween 20 (PBST), after which they were incubated with biotin-conjugated goat anti-llama antibodies (1:2000, Abcore) or mouse anti-histidine antibodies (1:2000, Thermo Fisher Scientific) at 37°C for 1 hour. After three washes with PBST, plates were incubated with streptavidin horseradish peroxidase (HRP; 1:10,000, Dako) or goat anti-mouse HRP (1:2000, Dako) at 37°C for 1 hour. After this incubation, plates were washed three times in PBST and incubated at room temperature for 10 min in the presence of 3,3′,5,5′-tetramethylbenzidine substrate (eBioscience). Reactions were stopped with 2N H_2SO_4 (Sigma). The absorbance of each sample was read at 450 nm with an ELISA reader (Tecan Infinite F200).

RNA isolation and cDNA synthesis

For RNA isolation, cryopreserved bone marrow cells were removed from the −135°C freezer and transferred to a 37°C water bath. The thawed cell suspension was quickly transferred to 40 ml of ice-cold RPMI 1640 (Lonza) medium. Cells were counted, and 10^7 cells were transferred to a new ribonuclease (RNase)–free falcon tube and centrifuged at room temperature at 300*g* for 10 min. The supernatant was completely removed, and cells were subsequently lysed with 1 ml of TRIzol reagent (Life Technologies) and 0.2 ml of RNase-free chloroform (Life Technologies). The mixture was vortexed for 15 s and incubated for 3 min at room temperature, followed by centrifugation at 13,000 rpm for 15 min at 4°C. The aqueous phase was transferred to a new tube. Subsequently, RNA was isolated using the RNeasy MinElute Cleanup Kit (Qiagen) according to the manufacturer's protocol. Total RNA was quantified at 260 nm using the NanoDrop 2000, and the quality of the isolated RNA sample was determined by measuring the A_{260}/A_{280} ratio. cDNA was synthesized from 1.5 µg of total RNA using a First-Strand cDNA Synthesis kit (Life Technologies). For a 20-µl reaction mix, 10 µl of RNA, 1 µl of deoxynucleoside triphosphate (dNTPs; 10 mM each), 1 µl of random hexamers (10 mM; Promega), and 1.5 µl of distilled water (dH_2O) were added to a microvial. The mixture was incubated at 65°C for 10 min and then at 4°C for 2 min. Next, 6.5 µl of reverse transcriptase mix containing 4 µl of 5× SuperScript III reaction buffer, 1 µl of dithiothreitol (100 mM), 0.5 µl of RNase inhibitor (20 U/µl), and 1 µl of SuperScript III reverse transcriptase (200 U/µl; Life Technologies) were added to the microvial and incubated at 25°C for 5 min, 50°C for 45 min, and 70°C for 20 min. cDNA was stored at 4°C until PCR amplification.

PCR amplification and cloning of VHH

The amplification of VHH was performed using a nested PCR approach (*29*) that was adapted for use with a high-fidelity DNA polymerase (PfuUltra II Fusion HS DNA Polymerase, Stratagene). The first PCR mix (50 µl of reaction volume) consisted of 5.0 µl of 10× PfuUltra II Fusion HS DNA polymerase buffer, 2.5 µl of dNTPs (10 mM each), 1.5 µl of gene-specific forward primer (CALL001, 5′-GTCCTGGCTGCTCTTCTACAAGG-3′; 10 mM), 1.5 µl of gene-specific reverse primer (CALL002, 5′-GGTACGTGCTGTTGAACTGTTCC-3′; 10 mM), 1.0 µl of PfuUltra II Fusion HS DNA polymerase, 36.5 µl of dH_2O, and 2.0 µl of cDNA. PCR amplification was performed in a thermocycler with the following protocol: initial denaturation at 94°C for 3 min, followed by 20 cycles at 94°C for 20 s, 50°C for 30 s, and 72°C for 2 min, and a final extension at 72°C for 10 min. The first PCR generated two amplified products: the heavy chain of conventional antibodies (~1000 bp) and the VHH heavy chain (~700 bp; fig. S1). The amplified VHH amplicon (~700 bp) was purified from the agarose gel using the QIAquick Gel Extraction Kit (Qiagen), according to the manufacturer's instructions. The product

was then subjected to the second round of PCR amplification using VHH inner primers that contained restriction sites for cloning: forward, 5′-CTAGTGCGGCCGCTGGAGACGGTGACCTGGGT-3′ (Eco 91I); reverse, 5′-GATGTGCAGCTGCAGGAGTCTGGRGGAGG-3′ (Pst I). PCR amplification continued for 12 to 14 cycles, after which the amplicons were purified with the QIAquick PCR Purification Kit (Qiagen) and digested using Eco 91I and Pst I. The vector pMES4 (GenBank accession number GQ907248) was digested with the same enzymes and dephosphorylated using alkaline phosphatase (New England Biolabs). VHH amplicons were ligated into pMES4 using a ratio of 100 ng of vector to 46 ng of VHH (~1:3 molar ratio). Next, we used *E. coli* strain WK6, prepared using the Mix & Go! *E. coli* Transformation Kit and Buffer Set (Zymo Research), for transformation according to the manufacturer's instructions. After transformation, cells were directly plated onto an ampicillin (100 μg/ml) nutrient agar plates. The following day, the insertion of VHH into the vector was confirmed by randomly picking 25 clones, screening by PCR for the insert, and Sanger sequencing, as described below.

Sequencing

To sequence the inserts, colony PCR was performed using PfuUltra II Fusion HS DNA Polymerase (Agilent Technologies) and primers (*29*) 5′-TTATGCTTCCGGCTCGTATG-3′ (MP57) and 5′-CCACAGACAGCCCTCATAG-3′ (GIII) under the following conditions: initial denaturation at 95°C for 3 min, followed by 39 cycles of (95°C for 20 s, 55°C for 30 s, and 72°C for 40 s), and a final extension at 72°C for 5 min. The amplicons were gel-purified and sequenced in both directions using the BigDye Terminator v3.1 Cycle Sequencing Kit and an ABI PRISM 3100 genetic analyzer (Applied Biosystems). The obtained sequences were assembled and aligned using CLC Genomics Workbench (CLC Bio 4.9).

SUPPLEMENTARY MATERIALS

Supplementary material for this article is available at http://advances.sciencemag.org/cgi/content/full/4/8/eaas9667/DC1

Supplementary Materials and Methods

Fig. S1. Direct cloning and expression of VHHs.

Fig. S2. VHHs block the interaction between the S1 protein and the MERS-CoV entry receptor DPP4.

Fig. S3. Amino acid sequences of VHH regions of anti–MERS-CoV spike VHHs.

Fig. S4. Phylogenetic tree of the amino acid sequences of the 46 MERS-CoV–neutralizing VHHs showing the corresponding neutralizing capacity of each VHH.

Fig. S5. Interaction of selected VHHs with recombinant MERS-CoV spike protein.

Fig. S6. Kinetics of VHH-1, VHH-4, VHH-83, and VHH-101 binding to MERS-CoV spike protein.

Fig. S7. Cross-competitive behavior of four different VHH-1, VHH-4, VHH-83, and VHH-101 determined using an Octet biosensor (ForteBio QK).

Fig. S8. Protective efficacy of MERS-CoV–specific VHHs in transgenic mice.

Table S1. Characteristics of MERS-CoV–specific VHHs.

Table S2. List of antibodies used in this study.

References (*47*–*52*)

REFERENCES AND NOTES

1. A. M. Zaki, S. van Boheemen, T. M. Bestebroer, A. D. M. E. Osterhaus, R. A. M. Fouchier, Isolation of a novel coronavirus from a man with pneumonia in Saudi Arabia. *N. Engl. J. Med.* **367**, 1814–1820 (2012).
2. S. Cauchemez, P. Nouvellet, A. Cori, T. Jombart, T. Garske, H. Clapham, S. Moore, H. L. Mills, H. Salje, C. Collins, I. Rodriquez-Barraquer, S. Riley, S. Truelove, H. Algarni, R. Alhakeem, K. AlHarbi, A. Turkistani, R. J. Aguas, D. A. T. Cummings, M. D. Van Kerkhove, C. A. Donnelly, J. Lessler, C. Fraser, A. Al-Barrak, N. M. Ferguson, Unraveling the drivers of MERS-CoV transmission. *Proc. Natl. Acad. Sci. U.S.A.* **113**, 9081–9086 (2016).
3. V. S. Raj, E. A. B. A. Farag, C. B. E. M. Reusken, M. M. Lamers, S. D. Pas, J. Voermans, S. L. Smits, A. D. M. E. Osterhaus, N. Al-Mawlawi, H. E. Al-Romaihi, M. M. AlHajri, A. M. El-Sayed, K. A. Mohran, H. Ghobashy, F. Alhajri, M. Al-Thani, S. A. Al-Marri, M. M. El-Maghraby, M. P. G. Koopmans, Bart L. Haagmans, Isolation of MERS coronavirus from a dromedary camel, Qatar, 2014. *Emerg. Infect. Dis.* **20**, 1339–1342 (2014).
4. M. Cotten, S. J. Watson, P. Kellam, A. A. Al-Rabeeah, H. Q. Makhdoom, A. Assiri, J. A. Al-Tawfiq, R. F. Alhakeem, H. Madani, F. A. AlRabiah, S. A. Hajjar, W. N. Al-nassir, A. Albarrak, H. Flemban, H. H. Balkhy, S. Alsubaie, A. L. Palser, A. Gall, Z. A. Memish, Transmission and evolution of the Middle East respiratory syndrome coronavirus in Saudi Arabia: A descriptive genomic study. *Lancet* **382**, 1993–2002 (2013).
5. X.-C. Tang, S. S. Agnihothram, Y. Jiao, J. Stanhope, R. L. Graham, E. C. Peterson, Y. Avnir, A. St. Clair Tallarico, J. Sheehan, Q. Zhu, R. S. Baric, W. A. Marasco, Identification of human neutralizing antibodies against MERS-CoV and their role in virus adaptive evolution. *Proc. Natl. Acad. Sci. U.S.A.* **111**, E2018–E2026 (2014).
6. D. Corti, J. Zhao, M. Pedotti, L. Simonelli, S. Agnihothram, C. Fett, B. Fernandez-Rodriguez, M. Foglierini, G. Agatic, F. Vanzetta, R. Gopal, C. J. Langrish, N. A. Barrett, F. Sallusto, R. S. Baric, L. Varani, M. Zambon, S. Perlman, A. Lanzavecchia, Prophylactic and postexposure efficacy of a potent human monoclonal antibody against MERS coronavirus. *Proc. Natl. Acad. Sci. U.S.A.* **112**, 10473–10478 (2015).
7. K. E. Pascal, C. M. Coleman, A. O. Mujica, V. Kamat, A. Badithe, J. Fairhurst, C. Hunt, J. Strein, A. Berrebi, J. M. Sisk, K. L. Matthews, R. Babb, G. Chen, K.-M. V. Lai, T. T. Huang, W. Olson, G. D. Yancopoulos, N. Stahl, M. B. Frieman, C. A. Kyratsous, Pre- and postexposure efficacy of fully human antibodies against Spike protein in a novel humanized mouse model of MERS-CoV infection. *Proc. Natl. Acad. Sci. U.S.A.* **112**, 8738–8743 (2015).
8. V. S. Raj, H. Mou, S. L. Smits, D. H. W. Dekkers, M. A. Müller, R. Dijkman, D. Muth, J. A. A. Demmers, A. Zaki, R. A. M. Fouchier, V. Thiel, C. Drosten, P. J. M. Rottier, A. D. M. E. Osterhaus, B. J. Bosch, B. L. Haagmans, Dipeptidyl peptidase 4 is a functional receptor for the emerging human coronavirus-EMC. *Nature* **495**, 251–254 (2013).
9. H. Mou, V. S. Raj, F. J. M. van Kuppeveld, P. J. M. Rottier, B. L. Haagmans, B. J. Bosch, The receptor binding domain of the new Middle East respiratory syndrome coronavirus maps to a 231-residue region in the spike protein that efficiently elicits neutralizing antibodies. *J. Virol.* **87**, 9379–9383 (2013).
10. S. S. Al-amri, A. T. Abbas, L. A. Siddiq, A. Alghamdi, M. A. Sanki, M. K. Al-Muhanna, R. Y. Alhabbab, E. I. Azhar, X. Li, A. M. Hashem, Immunogenicity of candidate MERS-CoV DNA vaccines based on the spike protein. *Sci. Rep.* **7**, 44875 (2017).
11. Y. Li, Y. Wan, P. Liu, J. Zhao, G. Lu, J. Qi, Q. Wang, X. Lu, Y. Wu, W. Liu, B. Zhang, K.-Y. Yuen, S. Perlman, G. F. Gao, J. Yan, A humanized neutralizing antibody against MERS-CoV targeting the receptor-binding domain of the spike protein. *Cell Res.* **25**, 1237–1249 (2015).
12. L. Jiang, N. Wang, T. Zuo, X. Shi, K.-M. V. Poon, Y. Wu, F. Gao, D. Li, R. Wang, J. Guo, L. Fu, K.-Y. Yuen, B.-J. Zheng, X. Wang, L. Zhang, Potent neutralization of MERS-CoV by human neutralizing monoclonal antibodies to the viral spike glycoprotein. *Sci. Transl. Med.* **6**, 234ra59 (2014).
13. A. S. Agrawal, T. Ying, X. Tao, T. Garron, A. Algaissi, Y. Wang, L. Wang, B.-H. Peng, S. Jiang, D. S. Dimitrov, C.-T. K. Tseng, Passive transfer of a germline-like neutralizing human monoclonal antibody protects transgenic mice against lethal Middle East respiratory syndrome coronavirus infection. *Sci. Rep.* **6**, 31629 (2016).
14. X. Yu, S. Zhang, L. Jiang, Y. Cui, D. Li, D. Wang, N. Wang, L. Fu, X. Shi, Z. Li, L. Zhang, X. Wang, Structural basis for the neutralization of MERS-CoV by a human monoclonal antibody MERS-27. *Sci. Rep.* **5**, 13133 (2015).
15. P. Chames, M. Van Regenmortel, E. Weiss, D. Baty, Therapeutic antibodies: Successes, limitations and hopes for the future. *Br. J. Pharmacol.* **157**, 220–233 (2009).
16. O. Spadiut, S. Capone, F. Krainer, A. Glieder, C. Herwig, Microbials for the production of monoclonal antibodies and antibody fragments. *Trends Biotechnol.* **32**, 54–60 (2014).
17. V. Irani, A. J. Guy, D. Andrew, J. G. Beeson, P. A. Ramsland, J. S. Richards, Molecular properties of human IgG subclasses and their implications for designing therapeutic monoclonal antibodies against infectious diseases. *Mol. Immunol.* **67**, 171–182 (2015).
18. C. Hamers-Casterman, T. Atarhouch, S. Muyldermans, G. Robinson, C. Hammers, E. B. Songa, N. Bendahman, R. Hammers, Naturally occurring antibodies devoid of light chains. *Nature* **363**, 446–448 (1993).
19. S. Muyldermans, Nanobodies: Natural single-domain antibodies. *Annu. Rev. Biochem.* **82**, 775–797 (2013).
20. E. De Genst, K. Silence, K. Decanniere, K. Conrath, R. Loris, J. Kinne, S. Muyldermans, L. Wyns, Molecular basis for the preferential cleft recognition by dromedary heavy-chain antibodies. *Proc. Natl. Acad. Sci. U.S.A.* **103**, 4586–4591 (2006).
21. U. Rothbauer, K. Zolghadr, S. Tillib, D. Nowak, L. Schermelleh, A. Gahl, N. Backmann, K. Conrath, S. Muyldermans, M. C. Cardoso, H. Leonhardt, Targeting and tracing antigens in live cells with fluorescent nanobodies. *Nat. Methods* **3**, 887–889 (2006).
22. G. Hassanzadeh-Ghassabeh, N. Devoogdt, P. De Pauw, C. Vincke, S. Muyldermans, Nanobodies and their potential applications. *Nanomedicine* **8**, 1013–1026 (2013).
23. F. Peyvandi, M. Scully, J. A. Kremer Hovinga, S. Cataland, P. Knöbl, H. Wu, A. Artoni, J. P. Westwood, M. Mansouri Taleghani, B. Jilma, F. Callewaert, H. Ulrichts, C. Duby, D. Tersago; TITAN Investigators, Caplacizumab for acquired thrombotic thrombocytopenic purpura. *N. Engl. J. Med.* **374**, 511–522 (2016).

24. P. Vanlandschoot, C. Stortelers, E. Beirnaert, L. I. Ibañez, B. Schepens, E. Depla, X. Saelens, Nanobodies®: New ammunition to battle viruses. *Antiviral Res.* **92**, 389–407 (2011).
25. E. A. B. A. Farag, C. B. E. M. Reusken, B. L. Haagmans, K. A. Mohran, V. Stalin Raj, S. D. Pas, J. Voermans, S. L. Smits, G.-J. Godeke, M. M. Al-Hajri, F. H. Alhajri, H. E. Al-Romaihi, H. Ghobashy, M. M. El-Maghraby, A. M. El-Sayed, M. H. J. Al Thani, S. Al-Marri, M. P. G. Koopmans, High proportion of MERS-CoV shedding dromedaries at slaughterhouse with a potential epidemiological link to human cases, Qatar 2014. *Infect. Ecol. Epidemiol.* **5**, 28305 (2015).
26. C. B. E. M. Reusken, B. L. Haagmans, M. A. Müller, C. Gutierrez, G.-J. Godeke, B. Meyer, D. Muth, V. Stalin Raj, L. Smits-De Vries, V. M. Corman, J.-F. Drexler, S. L. Smits, Y. E. El Tahir, R. De Sousa, J. van Beek, N. Nowotny, K. van Maanen, E. Hidalgo-Hermoso, M. P. G. Koopmans, Middle East respiratory syndrome coronavirus neutralising serum antibodies in dromedary camels: A comparative serological study. *Lancet Infect. Dis.* **13**, 859–866 (2013).
27. M. A. Müller, V. M. Corman, J. Jores, B. Meyer, M. Younan, A. M. Liljander, B.-J. Bosch, E. Lattwein, M. Hilali, B. E. Musa, S. Bornstein, S. S. Park, MERS coronavirus neutralizing antibodies in camels, Eastern Africa, 1983–1997. *Emerg. Infect. Dis.* **20**, 2093–2095 (2014).
28. B. L. Haagmans, J. M. A. van den Brand, V. Stalin Raj, A. Volz, P. Wohlsein, S. L. Smits, D. Schipper, T. M. Bestebroer, N. Okba, R. Fux, A. Bensaid, D. S. Foz, T. Kuiken, W. Baumgärtner, J. Segalés, G. Sutter, A. D. M. E. Osterhaus, An orthopoxvirus-based vaccine reduces virus excretion after MERS-CoV infection in dromedary camels. *Science* **351**, 77–81 (2016).
29. E. Pardon, T. Laeremans, S. Triest, S. G. F. Rasmussen, A. Wohlkönig, A. Ruf, S. Muyldermans, W. G. J. Hol, B. K. Kobilka, J. Steyaert, A general protocol for the generation of nanobodies for structural biology. *Nat. Protoc.* **9**, 674–693 (2014).
30. G. Hassanzadeh-Ghassabeh, D. Saerens, S. Muyldermans, in *Nanoproteomics*, S. A. Toms, R. J. Weil, Eds. (Humana Press, 2011), vol. 790, pp. 239–259.
31. R. Chakravarty, S. Goel, W. Cai, Nanobody: The "magic bullet" for molecular imaging? *Theranostics* **4**, 386–398 (2014).
32. N. Wang, X. Shi, L. Jiang, S. Zhang, D. Wang, P. Tong, D. Guo, L. Fu, Y. Cui, X. Liu, K. C. Arledge, Y.-H. Chen, L. Zhang, X. Wang, Structure of MERS-CoV spike receptor-binding domain complexed with human receptor DPP4. *Cell Res.* **23**, 986–993 (2013).
33. G. Lu, Y. Hu, Q. Wang, J. Qi, F. Gao, Y. Li, Y. Zhang, W. Zhang, Y. Yuan, J. Bao, B. Zhang, Y. Shi, J. Yan, G. F. Gao, Molecular basis of binding between novel human coronavirus MERS-CoV and its receptor CD26. *Nature* **500**, 227–231 (2013).
34. K. Li, C. Wohlford-Lenane, S. Perlman, J. Zhao, A. K. Jewell, L. R. Reznikov, K. N. Gibson-Corley, D. K. Meyerholz, P. B. McCray Jr., Middle East respiratory syndrome coronavirus causes multiple organ damage and lethal disease in mice transgenic for human dipeptidyl peptidase 4. *J. Infect. Dis.* **213**, 712–722 (2016).
35. F. I. Schmidt, L. Hanke, B. Morin, R. Brewer, V. Brusic, S. P. J. Whelan, H. L. Ploegh, Phenotypic lentivirus screens to identify functional single domain antibodies. *Nat. Microbiol.* **1**, 16080 (2016).
36. B. L. Haagmans, S. H. S. Al Dhahiry, C. B. E. M Reusken, V. Stalin Raj, M. Galiano, R. Myers, G.-J. Godeke, M. Jonges, E. Farag, A. Diab, H. Ghobashy, F. Alhajri, M. Al-Thani, S. A. Al-Marri, H. E. Al Romaihi, A. A. Khal, A. Bermingham, A. D. M. E. Osterhaus, M. P. G. Koopmans, Middle East respiratory syndrome coronavirus in dromedary camels: An outbreak investigation. *Lancet Infect. Dis.* **14**, 140–145 (2014).
37. A. Radbruch, G. Muehlinghaus, E. O. Luger, A. Inamine, K. G. C. Smith, T. Dörner, F. Hiepe, Competence and competition: The challenge of becoming a long-lived plasma cell. *Nat. Rev. Immunol.* **6**, 741–750 (2006).
38. J. I. Ellyard, D. T. Avery, T. G. Phan, N. J. Hare, P. D. Hodgkin, S. G. Tangye, Antigen-selected, immunoglobulin-secreting cells persist in human spleen and bone marrow. *Blood* **103**, 3805–3812 (2004).
39. E. Paramithiotis, M. D. Cooper, Memory B lymphocytes migrate to bone marrow in humans. *Proc. Natl. Acad. Sci. U.S.A.* **94**, 208–212 (1997).
40. R. A. Manz, A. E. Hauser, F. Hiepe, A. Radbruch, Maintenance of serum antibody levels. *Annu. Rev. Immunol.* **23**, 367–386 (2005).
41. V. K. Nguyen, R. Hamers, L. Wyns, S. Muyldermans, Camel heavy-chain antibodies: Diverse germline V_HH and specific mechanisms enlarge the antigen-binding repertoire. *EMBO J.* **19**, 921–930 (2000).
42. T. Ying, L. Du, T. W. Ju, P. Prabakaran, C. C. Y. Lau, L. Lu, Q. Liu, L. Wang, Y. Feng, Y. Wang, B.-J. Zheng, K.-Y. Yuen, S. Jiang, D. S. Dimitrov, Exceptionally potent neutralization of Middle East respiratory syndrome coronavirus by human monoclonal antibodies. *J. Virol.* **88**, 7796–7805 (2014).
43. D. Sok, K. M. Le, M. Vadnais, K. L. Saye-Francisco, J. G. Jardine, J. L. Torres, Z. T. Berndsen, L. Kong, R. Stanfield, J. Ruiz, A. Ramos, C.-H. Liang, P. L. Chen, M. F. Criscitiello, W. Mwangi, I. A. Wilson, A. B. Ward, V. V. Smider, D. R. Burton, Rapid elicitation of broadly neutralizing antibodies to HIV by immunization in cows. *Nature* **548**, 108–111 (2017).
44. E. A. F. Simões, J. P. DeVincenzo, M. Boeckh, L. Bont, J. E. Crowe Jr., P. Griffiths, F. G. Hayden, R. L. Hodinka, R. L. Smyth, K. Spencer, S. Thirstrup, E. E. Walsh, R. J. Whitley, Challenges and opportunities in developing respiratory syncytial virus therapeutics. *J. Infect. Dis.* **211** (Suppl. 1), S1–S20 (2015).
45. F. Song, R. Fux, L. B. Provacia, A. Volz, M. Eickmann, S. Becker, A. D. M. E. Osterhaus, B. L. Haagmans, G. Sutter, Middle East respiratory syndrome coronavirus spike protein delivered by modified vaccinia virus Ankara efficiently induces virus-neutralizing antibodies. *J. Virol.* **87**, 11950–11954 (2013).
46. V. S. Raj, M. M. Lamers, S. L. Smits, J. A. A. Demmers, H. Mou, B.-J. Bosch, B. L. Haagmans, in *Coronaviruses*, H. J. Maier, E. Bickerton, P. Britton, Eds. (Springer New York, 2015), vol. 1282, pp. 165–182.
47. H. Nakabayashi, K. Taketa, K. Miyano, T. Yamane, J. Sato, Growth of human hepatoma cells lines with differentiated functions in chemically defined medium. *Cancer Res.* **42**, 3858–3863 (1982).
48. S. van Boheemen, M. de Graaf, C. Lauber, T. M. Bestebroer, V. Stalin Raj, A. M. Zaki, A. D. M. E. Osterhaus, B. L. Haagmans, A. E. Gorbalenya, E. J. Snijder, R. A. M. Fouchier, Genomic characterization of a newly discovered coronavirus associated with acute respiratory distress syndrome in humans. *mBio* **3**, e00473-12 (2012).
49. S. L. Smits, A. de Lang, J. M. A. van den Brand, L. M. Leijten, W. F. van IJcken, M. J. C. Eijkemans, G. vanAmerongen, T. Kuiken, A. C. Andeweg, A. D. M. E. Osterhaus, B. L. Haagmans, Exacerbated innate host response to SARS-CoV in aged non-human primates. *PLOS Pathog.* **6**, e1000756 (2010).
50. F. J. van Kuppeveld, J. T. van der Logt, A. F. Angulo, M. J. van Zoest, W. G. Quint, H. G. Niesters, J. M. Galama, W. J. Melchers, Genus- and species-specific identification of mycoplasmas by 16S rRNA amplification. *Appl. Environ. Microbiol.* **58**, 2606–2615 (1992).
51. B. L. Haagmans, J. M. A. van den Brand, L. B. Provacia, V. Stalin Raj, K. J. Stittelaar, S. Getu, L. de Waal, T. M. Bestebroer, G. van Amerongen, G. M. G. M. Verjans, R. A. M. Fouchier, S. L. Smits, T. Kuiken, A. D. M. E. Osterhaus, Asymptomatic Middle East respiratory syndrome coronavirus infection in rabbits. *J. Virol.* **89**, 6131–6135 (2015).
52. Y. N. Abdiche, D. S. Malashock, A. Pinkerton, J. Pons, Exploring blocking assays using Octet, ProteOn, and Biacore biosensors. *Anal. Biochem.* **386**, 172–180 (2009).

Acknowledgments: We thank C. Vincke (Vrije Universiteit Brussel, Belgium) for providing the pMES4 plasmid and *E. coli* strain WK6 used to produce VHHs. We thank G. van Cappellen (Erasmus MC Optical Imaging Centre) for obtaining 96-well confocal pictures. We also thank the technical assistance of D. Solanes, X. Abad, I. Cordón, and all the animal caretakers from the CReSA BSL-3 animal facilities during the dromedary experiment. Evaluation of the protection of K18 mice was performed in CISA-INIA (Centro de Investigacion en Sanidad Animal – Instituto de Tecnologia Agraria y Alimentaria, Madrid, Spain). **Funding:** This study was financed by a grant from the Zoonotic Anticipation and Preparedness Initiative [ZAPI project; Innovative Medicines Initiative (IMI) grant agreement no. 115760], with the assistance and financial support of IMI and the European Commission, and in-kind contributions from European Federation of Pharmaceutical Industries and Associations partners. A part of the study was supported by the European Virus Archive Goes Global project, which received a grant from the European Union Horizon 2020 Framework Program for Research and Innovation (653316) and grants from the Ministry of Science and Innovation of Spain (Bio2016-75549-R AEI/FEDER, UE) and NIH (2PO1AIO6O699). **Author contributions:** V.S.R. and B.L.H. designed and coordinated the study. V.S.R., N.M.A.O., J.G.-A., D.D., B.v.D., W.W., M.M.L., I.W., R.F.-D., I.S., B.J.B., L.E., and B.L.H. performed laboratory experiments and analysis. A.B. and J.S. performed the camel experiments and obtained bone marrow samples. M.P.K. and A.D.M.E.O. supervised part of the experiments. V.S.R., N.M.A.O., and B.L.H. wrote the manuscript with comments from all authors. **Competing interests:** V.S.R., B.J.B., A.D.M.E.O., and B.L.H. are inventors on a patent application on MERS-CoV held by Erasmus MC (application no. 61/704,531, filed 23 September 2012, publication no. WO 2014/045254 A2). A.D.M.E.O. is the chief scientific officer of Viroclinics Biosciences BV. A.D.M.E.O. holds certificates of shares in Viroclinics Biosciences B.V. The authors declare no other competing interests. **Data and materials availability:** All data needed to evaluate the conclusions in the paper are present in the paper and/or the Supplementary Materials. The nucleotide sequences of the VHHs reported in this paper have been deposited in GenBank under accession numbers KX278382 to KX278416. The VHH-83 and HCAb-83 can be provided by EVAg pending scientific review and a completed material transfer agreement. Requests should be submitted on the EVAg website (www.european-virus-archive.com/).

Submitted 29 January 2018
Accepted 1 July 2018
Published 8 August 2018
10.1126/sciadv.aas9667

Citation: V. Stalin Raj, N. M. A. Okba, J. Gutierrez-Alvarez, D. Drabek, B. van Dieren, W. Widagdo, M. M. Lamers, I. Widjaja, R. Fernandez-Delgado, I. Sola, A. Bensaid, M. P. Koopmans, J. Segalés, A. D. M. E. Osterhaus, B. J. Bosch, L. Enjuanes, B. L. Haagmans, Chimeric camel/human heavy-chain antibodies protect against MERS-CoV infection. *Sci. Adv.* **4**, eaas9667 (2018).

Science Advances

Chimeric camel/human heavy-chain antibodies protect against MERS-CoV infection

V. Stalin Raj, Nisreen M. A. Okba, Javier Gutierrez-Alvarez, Dubravka Drabek, Brenda van Dieren, W. Widagdo, Mart M. Lamers, Ivy Widjaja, Raul Fernandez-Delgado, Isabel Sola, Albert Bensaid, Marion P. Koopmans, Joaquim Segalés, Albert D. M. E. Osterhaus, Berend Jan Bosch, Luis Enjuanes and Bart L. Haagmans

Sci Adv **4** (8), eaas9667.
DOI: 10.1126/sciadv.aas9667